NBS-GCR-88-542

Thermal Cracking and Variable Properties Effects on Free Boundary Layer Diffusion Flames

Thomas George Matage

March 1988

Sponsored by
U.S. DEPARTMENT OF COMMERCE
National Bureau of Standards
National Engineering Laboratory
Center for Fire Research
Gaithersburg, MD 20899

NBS-GCR-88-542

THERMAL CRACKING AND VARIABLE PROPERTIES EFFECTS ON FREE BOUNDARY LAYER DIFFUSION FLAMES

Thomas George Matage

University of California
Berkeley, CA

March 1988

Grant Number 60NANB5D0552

Sponsored by
U.S. DEPARTMENT OF COMMERCE
National Bureau of Standards
National Engineering Laboratory
Center for Fire Research
Gaithersburg, MD 20899

Notice

This report was prepared for the Center for Fire Research of the National Engineering Laboratory, National Bureau of Standards Under Grant Number 60NANB5D0552. The Statements and Conclusions contained in this report are those of the authors and do not necessarily reflect the views of the National Bureau of Standards or the Center for Fire Research.

Thermal Cracking and Variable Properties Effects
on Free Boundary Layer Diffusion Flames

By

Thomas George Mataga

B.S. (University of California) 1984

THESIS

Submitted in partial satisfaction of the requirements for the degree of

MASTER OF SCIENCE

in

ENGINEERING

in the

GRADUATE DIVISION

of the

UNIVERSITY OF CALIFORNIA, BERKELEY

Approved: Patrick J. Pagni 12/16/86
Chairman Date

A. C. F. Kelly 12/9/86

Robert F. Sawyer 12/15/86

Contents

I. Introduction	1
II. Analysis	3
A. Governing equations	3
B. Assumptions	7
C. Modified Shvab Zeldovich Variables	8
D. Species and Enthalpy Fields	12
E. Treatment of Boundary Layer Equations	14
F. Simplified Governing Equations	16
G. Outline of Solution	17
III. Discussion and Results	19
A. Fuels Modeled	19
B. Experimental Results	23
C. Pyrolysis Rates	25
D. Parametric Studies	25
IV. Conclusion	26
V. Nomenclature	27
VI. Figure Captions	31
VII. References	33

I. Introduction

This paper presents an analytical model for a free convective boundary layer diffusion flame and compares results from this model to experiment. The analytical model will add two new features to the solution presented by Pagni[1] in order to improve agreement with experimental data [2]. The analysis builds upon the work originally done by Kosdon, Williams, and Buman [3]; and Kim, de Ris, and Krosser [4]. It is proposed that the fuel undergoes endothermic decomposition before reaching the flame. Several experimental studies have demonstrated this phenomena [5,6,7]. The endothermic decomposition of the fuel will be referred to as cracking. The effect of cracking on the free convective diffusion flame is explored by the use of modified Shvab Zeldovich variables which model both the flame reaction and the cracking reaction [8]. The second addition to the solution given by Pagni is the use of a temperature dependent density-viscosity ($\rho\mu$) function [9] which allows the ambient viscosity to be determined by ambient conditions. In order to match the location of the theoretical flame with the location of the experimental flame, previous studies [10] have adjusted the ambient viscosity to non ambient values. By using the temperature dependent density-viscosity ($\rho\mu$) function, the analytical model accurately predicts the location of the flame using the ambient value of viscosity.

Figure 1 shows a schematic diagram of the free convective diffusion flame. The wall is a pyrolyzing slab from which fuel is endothermically pyrolyzed by heat flux to the wall. The fuel then diffuses toward the flame.

At a sufficiently high temperature the fuel undergoes an endothermic reaction in which the fuel molecules decompose into simpler molecules. This reaction zone will be modeled as a sheet in order to simplify the analysis. The actual cracking reaction occurs over a fairly wide region. The cracked fuel then diffuses toward the flame and toward the wall. Cracked fuel reaching the flame burns in an exothermic reaction with oxygen generating products and providing heat to drive both the flow and the combustion process.

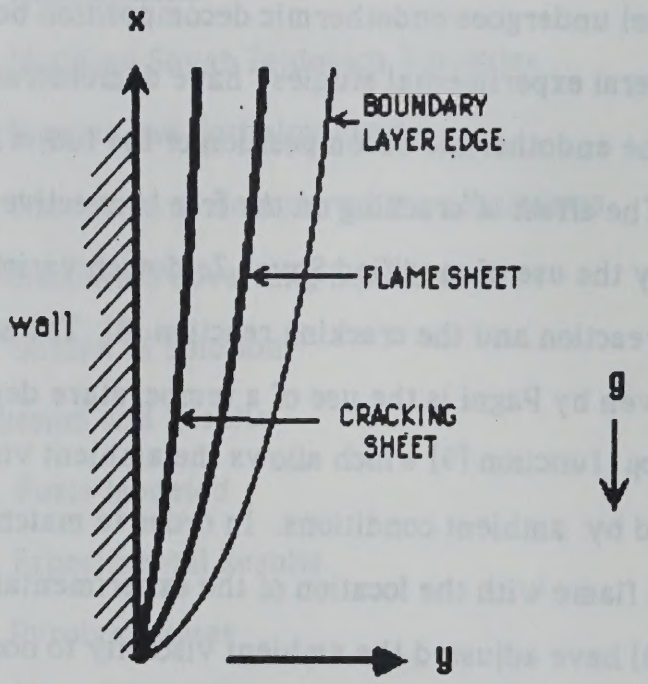

Fig. 1.

The analysis of the flame incorporating the effects of thermal cracking and temperature dependent density viscosity product ($\rho\mu$) occupies the first half of the paper. The analysis begins with the governing equations and their boundary conditions. Following this, the assumptions used to simplify the governing equations are given. The analysis proceeds with the

derivation of the modified Shvab Zeldovich variables used to eliminate the generation terms in the energy and species equations. The determination of enthalpy and species fields necessary for the solution of the problem are presented next. Nondimensional groups describing the flow field are then introduced which include a Howarth-Dorodnitzyn transformation to make the governing equations appear incompressible. The variable properties are introduced at this point. The problem is reduced from two dimensions to one dimension through the use of a similar stream function. The governing equations are then restated in their simplified form. Six nondimensional groups are shown to describe the system.

The second half of the paper examines the results of the analytical model. Solutions with and without cracking are compared with experimental data [2] for temperature and streamwise velocity. The fuels modeled are cyclohexane, ethanol, iso-octane, and n-heptane. The pyrolysis rate at the wall is predicted for each of the fuels based on the theoretical results. Finally, the nondimensional groups describing the cracking reaction are varied in a parametric study to determine there effect on the flame solution.

II. Analysis

A. Governing Equations

Symbols are defined in the nomenclature. The flame is assumed to be steady and two dimensional with coordinate system shown in figure 1. With the addition of fuel cracking, the one step reaction,

$$\nu_{F_1} F_1 + \nu_o O \longrightarrow \nu_p P + Q_{FL}, \qquad (1)$$

is broken up into two reactions. The first reaction is the cracking reaction :

$$\nu_{F1} F_1 \longrightarrow \nu_{F2} F_2 - Q_{CR} \quad . \tag{2}$$

And the second reaction is the modified flame reaction in which the cracked fuel reacts with the oxidizer:

$$\nu_{F2} F_2 + \nu_O O \longrightarrow \nu_P P + Q_{CRFL} \quad . \tag{3}$$

The enthalpies of reaction are related by

$$Q_{CRFL} = Q_{FL} + Q_{CR} \quad . \tag{4}$$

In the analysis only Q_{cr} and Q_{fl} will be used. Where Q_{crfl} is needed, the right hand side of eqn. (4) will be used.

The conservation equations and boundary conditions are as follows. Conservation of mass :

$$\nabla \cdot (\rho \underset{\sim}{v}) = 0 \quad . \tag{5}$$

Conservation of momentum :

$$\rho \underset{\sim}{v} \cdot \nabla \underset{\sim}{v} - \nabla \cdot (\mu \nabla \underset{\sim}{v}) = \underset{\sim}{g}(\rho - \rho_\infty) - \nabla p \tag{6}$$

with boundary conditions for streamwise velocity given by

$$u(x,0) = u(0,y) = u(x,\infty) = 0 \quad . \tag{7}$$

The boundary conditions for transverse velocity account for the blowing at the wall.

$$v(x,0) = \frac{\dot{m}''_w}{\rho_w} \quad \text{and} \quad v(0,y) = v(x,\infty) = 0. \tag{8}$$

Conservation of energy :

$$\rho \underset{\sim}{v} \cdot \nabla h - \nabla \cdot \left(\frac{\lambda}{c_p} \nabla h \right) = \dot{q}'''_{FL} + \dot{q}'''_{CR} \qquad (9)$$

where

$$h \equiv \int_{T_\infty}^{T} c_p \, dT \, . \qquad (10)$$

The energy equation contains two source terms. The first term, $\dot{q}''_{FL}$, represents the heat produced by the flame reaction. The second source term, $\dot{q}''_{CR}$ accounts for the energy absorbed by the cracking reaction. The boundary conditions for the energy equation are

$$h(x,0) = h_w \quad \text{and} \quad h(0,y) = h(x,\infty) = 0 \, . \qquad (11)$$

The species equation must be solved for the uncracked fuel (Y_{f1}), the cracked fuel (Y_{f2}), and the oxidizer (Y_o). The species equation for Y_o is

$$\rho \underset{\sim}{v} \cdot \nabla Y_o - \nabla \cdot (\rho D Y_o) = \dot{m}'''_o \qquad (12)$$

with boundary conditions

$$Y_o(x,0) = 0 \quad \text{and} \quad Y_o(0,y) = Y_o(x,\infty) = Y_{o\infty} \, . \qquad (13)$$

The uncracked fuel species equation is

$$\rho \underset{\sim}{v} \cdot \nabla Y_{f1} - \nabla \cdot (\rho D Y_{f1}) = \dot{m}'''_{f1CR} \qquad (14)$$

where $\dot{m}'''_{f1CR}$ represents the mass sink of uncracked fuel at the cracking

sheet. Ambient boundary conditions for the uncracked fuel are homogeneous. The wall boundary condition is determined by a mass balance at the wall where Y_{FT} is used to account for the inerts in the pyrolyzed material.

$$\dot{m}''_w Y_{FT} = \dot{m}''_w Y_{f1w} - \rho D \frac{\partial Y_{f1}}{\partial n}\Big|_w . \qquad (15)$$

The cracked fuel species equation is

$$\rho \underline{v} \cdot \nabla Y_{f2} - \nabla \cdot (\rho D Y_{f2}) = \dot{m}'''_{f2CR} + \dot{m}'''_{f2FL} \qquad (16)$$

where $\dot{m}'''_{f2CR}$ is a source of cracked fuel at the cracking reaction, and $\dot{m}'''_{f2FL}$ is a sink of cracked fuel at the flame reaction. Ambient boundary conditions for the cracked fuel are also homogeneous. The wall boundary condition for cracked fuel assumes that the cracked fuel does not diffuse into the wall.

$$\dot{m}''_w Y_{f2w} = \rho D \frac{\partial Y_{f2}}{\partial n}\Big|_w . \qquad (17)$$

An energy balance at the wall determines the wall mass flux.

$$\dot{m}''_w L = \frac{\lambda}{c_p} \frac{\partial h}{\partial n} . \qquad (18)$$

This completes the list of governing equations. The introduction of the variable properties will be introduced when the equations are nondimensionalized.

B. Assumptions

The following are a list of simplifications and assumptions used in the analytic model.

1. The flow is assumed to be steady, laminar, and two dimensional.

2. Diffusion is governed by Fick's Law with the same diffusion coefficients for all species.

2. The overall reaction will be modeled as a two step reaction: a flame reaction and a cracking reaction occurring at two separate regions in the boundary layer.

3. The flame reaction zone and the cracking reaction zone will be modeled as sheets.

4. All undecomposed fuel which reaches the cracking sheet will be assumed to decompose fully and irreversibly into cracked fuel.

5. The cracked fuel cannot diffuse into the pyrolyzing slab.

6. Cracked fuel and oxygen are completely consumed in stoichiometric proportions at the flame sheet to form products.

7. The cracking reaction takes place at a known temperature.

8. The Lewis number equals one.

9. Specific heat is not a function of temperature.

10. The density viscosity product is modeled using the viscosity of Nitrogen.

11. The wall temperature is the boiling temperature of the fuel at atmospheric pressure.

12. Assume a similar solution.

13. Neglect radiation.

14. Ambient is at rest.

C. Modified Shvab Zeldovich Variables

The first step in the analysis is the removal of the generation terms in the energy and species equations. By assuming unity Lewis number and stoichiometric consumption of species, it is possible to eliminate the generation terms by using modified Shvab Zeldovich variables. The treatment of multiple flame sheets by the use of Shvab Zeldovich variables was originally developed by Penner and Libby [8]. Equation (2) limits the consumption of energy and species at the cracking sheet to

$$\frac{-\dot{m}'''_{f1}}{\nu_F M_F} = \frac{\dot{m}'''_{f2CR}}{\nu_F M_F} = \frac{-\dot{q}'''_{CR}}{Q_{CR}} \quad . \tag{19}$$

Similarly, Equation (3) limits the consumption of energy and species at the flame sheet to $\frac{-\dot{m}'''_{f2FL}}{\nu_F M_F} = \frac{-\dot{m}'''_{o}}{\nu_o M_o} = \frac{\dot{q}'''_{FL}}{Q_{FL} + Q_{CR}}$. (20)

By using eqns. (19) and (20), the species equation for Y_o, Y_{f1}, and Y_{f2} can be reduced to a single, homogeneous equation with the independent variable

$$\beta \equiv \frac{Y_{f1}}{\nu_F M_F} + \frac{Y_{f2}}{\nu_F M_F} - \frac{Y_o}{\nu_o M_o} \quad . \tag{21}$$

This variable is normalized such that the boundary conditions are either unity or zero by

$$J \equiv \frac{\beta - \beta_\infty}{\beta_w - \beta_\infty} \quad . \tag{22}$$

The species mass fractions are nondimensionalized by the ambient mass fraction of oxygen and the stoichiometric ratio

$$\tilde{Y}_{F1} \equiv \frac{Y_{f1}}{Y_{o\infty}} \frac{\nu_o M_o}{\nu_F M_F} \quad , \quad \tilde{Y}_{F2} \equiv \frac{Y_{f2}}{Y_{o\infty}} \frac{\nu_o M_o}{\nu_F M_F} \quad \text{and} \quad \tilde{Y}_o \equiv \frac{Y_o}{Y_{o\infty}} \quad . \tag{23}$$

The nondimensional uncracked fuel at the wall will be referred to as the

uncracked fuel equivalence ratio

$$\phi_{F1} \equiv \frac{Y_{F1w}}{Y_{O\infty}} \frac{\nu_O M_O}{\nu_F M_F} \quad . \tag{24}$$

The cracked fuel at the wall will be refered to as the cracked fuel equivalence ratio

$$\phi_{F2} \equiv \frac{Y_{F2w}}{Y_{O\infty}} \frac{\nu_O M_O}{\nu_F M_F} \quad . \tag{25}$$

These variables are unknown at this point. Using the nondimensional variables, the normalized Shvab Zeldovich variable becomes

$$J = \frac{\tilde{Y}_{F1} + \tilde{Y}_{F2} - \tilde{Y}_O + 1}{\phi_{F1} + \phi_{F2} + 1} \quad , \tag{26}$$

and the species equation reduces to

$$\rho \underline{v} \cdot \nabla J - \nabla \cdot (\rho D \nabla J) = 0 \tag{27}$$

with boundary conditions

$$J(x,0) = 1 \quad \text{and} \quad J(0,y) = J(x,\infty) = 0 \quad . \tag{28}$$

The generation term in the energy equation is eliminated using the following independent variable

$$\gamma \equiv \frac{h}{Q_{FL} + Q_{CR}} + \frac{Y_O}{\nu_O M_O} \frac{Q_{FL}}{Q_{FL} + Q_{CR}} + \frac{Y_{F2}}{\nu_F M_F} \frac{Q_{CR}}{Q_{FL} + Q_{CR}} \quad . \tag{29}$$

This variable is normalized such that

$$J \equiv \frac{\gamma - \gamma_\infty}{\gamma_w - \gamma_\infty} = \frac{\beta - \beta_\infty}{\beta_w - \beta_\infty} \quad . \tag{30}$$

With the specific heat assumed constant, the enthalpy is

$$h = c_p (T - T_\infty) \quad . \tag{31}$$

The ambient oxygen and the heat released by the overall flame reaction are used to nondimensionalize the enthalpy so that the dimensionless enthalpy is defined as

$$\tilde{h} \equiv \frac{c_p (T - T_\infty) \nu_o M_o}{Q_{FL} Y_{o\infty}} \quad . \tag{32}$$

This variable is of order one at the flame. The dimensionless enthalpy at the wall is defined using eqn. (32) as $\tilde{h}_w \equiv \frac{c_p (T_w - T_\infty) \nu_o M_o}{Q_{FL} Y_{o\infty}}$. (33)

The ratio of the cracking enthalpy of reaction to the overall enthalpy of reaction indicates the relative magnitude of the heat absorbed by the cracking reaction and is defined as

$$\tilde{Q} \equiv \frac{Q_{CR}}{Q_{FL}} \quad . \tag{34}$$

Using the previously defined nondimensional groups, the normalized energy species variable as defined by eqn. (30) becomes

$$J = \frac{\tilde{h} + \tilde{Y}_o + \tilde{Y}_{F2} \tilde{Q} - 1}{\tilde{h}_w + \phi_{F2} \tilde{Q} - 1} \quad . \tag{35}$$

The differential equation for the energy species variable is eqn. (27) with boundary conditions given by eqn. (28).

In the solution to the problem with cracking, the parameters used to normalize the species and the energy species variables (Y_{f1w} ,Y_{f2w}) are variables. In the solution of the problem without cracking, these parameters could be determined *a priori* by the mass transfer number,B , and the mass

fraction of fuel in the transferred gas, Y_{FT}. The existence of the endothermic cracking sheet causes the mass fraction of uncracked fuel at the wall to be dependent upon both the mass fraction of cracked fuel at the wall and the heat absorbed by the cracking sheet. The traditional mass transfer number is defined as

$$B \equiv \left[\frac{Y_{o\infty} Q_{FL}}{v_o M_o} - h_w \right] / L \quad , \qquad (36)$$

and the nondimensional fuel in transferred medium is defined as

$$\phi_{FT} \equiv \frac{Y_{FT} v_o M_o}{Y_{o\infty} v_F M_F} \quad . \qquad (37)$$

For the problem <u>without</u> cracking, ϕ_{f1} is determined by the energy and mass balance at the wall to be

$$\phi_{F1} = \frac{\phi_{FT} B - 1}{B + 1} \quad . \qquad (38)$$

With the addition of cracking, the mass transfer number is modified by a cracking mass transfer number defined as

$$B_{CR} \equiv \frac{Y_{f2w} Q_{CR}}{v_F M_F L} \quad . \qquad (39)$$

An effective mass transfer number is then defined as

$$B_{eff} \equiv \frac{B - B_{CR}}{1 + B_{CR}} \quad . \qquad (40)$$

The value of ϕ_{f1} is determined by eqn (15), eqn (17) , and eqn(18) for the energy and mass balances at the wall and eqn. (26) and eqn. (35) for the definitions of the Shvab Zeldovich variables giving

$$\phi_{F1} + \phi_{F2} = \frac{\phi_{FT} B_{eff} - 1}{B_{eff} + 1} \quad . \qquad (41)$$

The value of ϕ_{f2} is still unknown and must be determined by the solution of the cracked fuel species equation inside the cracking sheet.

D. Species and Enthalpy Fields

In order to solve for the species and enthalpy fields, it is necessary to solve the differential equation for J. A system of iteration is needed since the solution for J is dependent upon the enthalpy field through the momentum equation. In this section, it is assumed that the solution for J is known. The following results rely on the assumption that all species diffusing toward either the flame sheet or cracking sheet are completely consumed. From the cracking sheet to the ambient environment there are only two field variables present: either the cracked fuel and enthalpy, or the oxidizer and enthalpy. Since there are two independent Shvab Zeldovich variables and only two field variables, the enthalpy and species fields are completely specified by the solution to J. Between the cracking sheet and the wall, both the cracked fuel and the uncracked fuel are present with the enthalpy. Since there are three field variables and only two Shvab Zeldovich variables, it is necessary to solve the species equation for the cracked fuel in the region between the cracking sheet and the wall.

The location of the cracking sheet is specified by the temperature at which the cracking reaction occurs. It is also know that the mass fraction of the uncracked fuel goes to zero at the cracking sheet. The location of the cracking sheet in the solution for J is found from this information. With the assumption of constant specific heat, the dimensionless enthalpy at the

cracking sheet defined as

$$\tilde{h}_{CR} \equiv \frac{C_p (T_{CR} - T_\infty) V_0 M_0}{Q_{FL} Y_{O\infty}} \quad . \qquad (42)$$

The location of the cracking sheet in J is determined from the species and the energy species variables as

$$J_{CR} \equiv \frac{1 + \tilde{Q} - \tilde{h}_{CR}}{1 + \tilde{Q} + \phi_{FL} \tilde{Q} - \tilde{h}_w} \quad . \qquad (43)$$

By solving the species variable for $\tilde{y}_{f2}$ and using the location of the cracking sheet in J, it is then possible to determine the value of y_{f2cr} at the cracking sheet:

$$\tilde{y}_{F2CR} \equiv J_{CR} [\phi_{F1} + \phi_{F2} + 1] - 1 \quad . \qquad (44)$$

The boundary conditions for the cracked fuel species equation are now completely specified by the zero flux condition at the wall, eqn.(17), and the value of $\tilde{y}_{f2cr}$ at the cracking sheet, eqn.(44).

The location of the flame sheet in J is found by setting y_0 and y_{f2} equal to zero so that eqn. (26) reduces to

$$J_{FL} \equiv \frac{1}{\phi_{F1} + \phi_{FL} + 1} \quad . \tag{45}$$

The location of the flame sheet in J separates the region in which the oxidizer is zero from the region in which the cracked fuel is zero. With this information it now possible to determine the enthalpy field. The enthalpy between the cracking sheet and the wall is determined by

$$\tilde{h} = 1 - \tilde{y}_{FL}\,\tilde{Q} - J\,[1 - \phi_{FL}\,\tilde{Q} - \tilde{h}_w] \,. \tag{46}$$

The enthalpy between the cracking sheet and the flame sheet is given by

$$\tilde{h} = 1 + \tilde{Q} - J\,[1 + \tilde{Q} + \phi_{FL}\,\tilde{Q} - \tilde{h}_w] \,, \tag{47}$$

and enthalpy from the flame sheet to ambient is

$$h = J\,[\phi_{F1} + \phi_{F2}\,(1 + \tilde{Q}) + \tilde{h}_w] \,. \tag{48}$$

E. Treatment of the Boundary Layer Equations

The treatment of the boundary layer equations follows that given in previous work [2] except for the addition of a temperature dependent density viscosity product ($\rho\mu$). The density viscosity product is determined using the viscosity of nitrogen and is calculated using the collision integrals for a Leonard-Jones potential given in Hirschfelder, Curtis and Bird [9]. Curve fitting density viscosity product with T / T_{inf} yields

$$\alpha \equiv \left(\frac{\rho\mu}{\rho_\infty \mu_\infty}\right) = \left(\frac{T}{T_\infty}\right)^{-0.325} \,. \tag{49}$$

The boundary layer equations for J and the cracked fuel are the same. For the cracked fuel equation, J is replaced by $\tilde{y}_{f2}$.

$$\rho u \frac{\partial J}{\partial x} + \rho v \frac{\partial J}{\partial y} = \frac{\partial}{\partial y}\left(\rho D \frac{\partial J}{\partial y}\right) . \qquad (50)$$

The momentum equation is

$$\rho u \frac{\partial u}{\partial x} + \rho v \frac{\partial u}{\partial y} = \frac{\partial}{\partial y}\left[\mu \frac{\partial u}{\partial y}\right] - \frac{\partial p}{\partial x} - g(\rho - \rho_\infty) . \qquad (51)$$

A Howarth-Dorodnitzyn transform is used to make the governing equations appear incompressible. The nondimensional variables used to describe the flow field are given as,

$$\xi \equiv \frac{x}{\ell} \quad , \quad S \equiv \frac{Gr_\ell^{1/4}}{\ell} \int_0^y \frac{\rho}{\rho_\infty} dy \quad , \qquad (52)$$

$$U \equiv \frac{u\ell}{Gr_\ell^{1/2} \nu_\infty} \quad \text{and} \quad V \equiv \frac{\ell}{Gr_\ell^{1/2} \rho_\infty \nu_\infty}\left(\rho v + u \int_0^y \frac{\partial \rho}{\partial x} dy\right) .$$

Using these groups, eqns. (5), (50), and (51) become

$$\frac{\partial U}{\partial \xi} + \frac{\partial V}{\partial S} = 0 \quad , \qquad (53)$$

$$U \frac{\partial J}{\partial \xi} + V \frac{\partial J}{\partial S} = \frac{1}{Pr} \frac{\partial}{\partial S}\left[\alpha \frac{\partial J}{\partial S}\right] \quad , \qquad (54)$$

$$U \frac{\partial U}{\partial \xi} + V \frac{\partial U}{\partial S} = \frac{\partial}{\partial S}\left[\alpha \frac{\partial U}{\partial S}\right] + \frac{T - T_\infty}{T_w - T_\infty} . \qquad (55)$$

A stream function is used to satisfy conservation of mass.

$$U \equiv \frac{\partial \psi}{\partial S} \quad \text{and} \quad V \equiv -\frac{\partial \psi}{\partial \xi} . \qquad (56)$$

The solution is assumed to be similar by the use of a similar stream function

$$\psi \equiv (4\xi)^{3/4} f(\eta) \quad , \qquad (57)$$

and a similarity variable defined as

$$\eta = \frac{\xi}{(4\xi)^{1/4}} \quad . \qquad (58)$$

This reduces the problem from two dimensions to only one dimension.

F. Reduced Governing Equations

The governing equations can now be restated in there reduced form. The differential equation for the energy species variable is given as

$$[\alpha J']' + Pr\, f\, J' = 0 \quad , \qquad (59)$$

with boundary conditions

$$J(0) = 1 \quad \text{and} \quad J(\infty) = 0 \quad . \qquad (60)$$

The cracked fuel species equation inside the cracking sheet is specified by

$$[\alpha \tilde{Y}_{F2}']' + Pr\, f\, \tilde{Y}_{F2}' = 0 \qquad (61)$$

with the zero flux into the wall condition given as

$$3\, Pr\, f(0)\, \tilde{Y}_{F2w} = \left.\frac{\partial \tilde{Y}_{F2}}{\partial \eta}\right|_{\eta=0} \qquad (62)$$

and the boundary condition at the cracking sheet given by

$$\tilde{Y}_{F2}(\eta_{CR}) = \tilde{Y}_{F2CR} \quad . \qquad (63)$$

where eqn. (44) is used to determine $\tilde{y}_{F_2 cr}$. The value of η_{cr} is found by searching the solution of $J(\eta)$ for J_{cr} as specified by eqn. (43). A similar method is used to find η_{ff}. The reduced momentum equation is

$$[\alpha f'']' + 3 f f'' - 2(f')^2 + \frac{\tilde{h}}{\tilde{h}_u} = 0, \quad (64)$$

with boundary conditions

$$f'(0) = 0 \quad \text{and} \quad f'(\infty) = 0 \quad . \quad (65)$$

The blowing condition at the wall is given by

$$3 Pr\, f(0) = B_{eff} \left.\frac{\partial T}{\partial n}\right|_{n=0} \quad (66)$$

where B_{eff} is defined by eqn(40). The enthalpy field is given by eqn. (46), (47), and (48).

G. Outline of Solution

The system of equations are highly coupled and must be solved in an iterative manner. The equations that must be solved are as follows: Equations (59) through (66) give the governing equations and main boundary conditions; eqns. (43) through (49) determine the enthalpy field, the density viscosity product and one of the boundary conditions for the cracked fuel equation; and eqns. (39) through (41) determine the effective mass transfer number and the uncracked fuel equivalence ratio.

The diffusion flame with cracking is controlled by six nondimensional parameters listed in table 1. Besides these parameters, the Prandtl number and the ambient properties of air must be known. The effect of cracking adds two new parameters to the analysis: the heat of reaction ratio gives the ratio of the cracking heat of reaction to the total heat of reaction and

indicates the relative amount of heat absorbed by the cracking sheet. The cracking enthalpy determines the location of the cracking sheet in the enthalpy field.

The problem is solved numerically using the C programing language. The momentum equation is linearized and solved using a tridiagonal solver. The energy-species equation and cracked fuel equation are solved using separation of variables and integration. The complex interdependencies are solved by iteration.

TABLE 1

Summary of Dimensionless Parameters

Fuel in Transferred medium

$$\phi_{FT} \equiv \frac{Y_{FT}}{Y_{o\infty}} \frac{v_o M_o}{v_F M_F}$$

Mass transfer number

$$B \equiv \left[\frac{Q_{FL} Y_{o\infty}}{v_o M_o} - h_w \right] / L$$

Wall enthalpy

$$\tilde{h}_w \equiv \frac{c_p (T_w - T_\infty) v_o M_o}{Q_{FL} Y_{o\infty}}$$

Cracking enthalpy

$$\tilde{h}_{CR} \equiv \frac{c_p (T_{CR} - T_\infty) v_o M_o}{Q_{FL} Y_{o\infty}}$$

Heat of reaction ratio

$$\tilde{Q} \equiv \frac{Q_{CR}}{Q_{FL}}$$

Grashof number evaluated at ℓ

$$Gr_\ell \equiv \frac{g (T_w - T_\infty) \ell^3}{v_\infty^2 T_\infty}$$

Discussion and Results

A. Fuels Modeled

The fuels chosen for analysis were based on the availability of experimental data for temperature and velocity [2] fields. The fuels modeled were n-heptane, iso-octane, cyclohexane, and ethanol. The general overall reaction for these fuels can be written as

$$\nu_{F_1} F_1 + \nu_{O_2} O_2 \rightarrow \nu_{CO_2} CO_2 + \nu_{H_2O} H_2O + Q_{FL} \quad (67)$$

where the stoichiometric coefficients, the fuel molecules, and the enthalpies of reaction are given in table 2. At the cracking reaction, the fuels were assumed to decompose into acetylene (C_2H_2), hydrogen (H_2) and carbon monoxide (CO). The choice of acetylene was based on species profiles given for a methane air diffusion flame[12]. Of the intermediate hydrocarbons, acetylene was measured to have the highest concentration. The general cracking reaction is

$$\nu_{F_1} F_1 \rightarrow \nu_{C_2H_2} C_2H_2 + \nu_{H_2} H_2 + \nu_{CO} CO - Q_{CR}, \quad (68)$$

with fuel molecules, enthalpies of reaction, and stoichiometric coefficients given in table 3. Note that the reaction is endothermic when Q_{cr} is greater than zero. The reaction at the flame is then given as

$$\nu_{C_2H_2} C_2H_2 + \nu_{H_2} H_2 + \nu_{CO} CO + \nu_{O_2} O_2 \rightarrow \nu_{CO_2} CO_2 + \nu_{H_2O} H_2O + Q_{FL} + Q_{CR}. \quad (69)$$

This is a very simple approximation to the flame chemistry and will probably be improved in the future. But even though it is simple, it will be shown to give good results.

TABLE 2
Constants for One Step Reaction

fuel	molecule	ν_{f1}	ν_{O}	ν_{CO2}	ν_{H2O}	Q_{f1} (J/kmol)
cyclohexane	C_6H_{12}	1	9	6	6	3.689e+09
n-Heptane	C_7H_{16}	1	11	7	8	4.501e+09
Iso-Octane	C_8H_{18}	1	12.5	8	9	5.100e+09
Ethanol	C_2H_6O	1	3	2	3	1.235e+09

TABLE 3
Constants for the Decomposition of Fuel into Acetylene

fuel	molecule	ν_{f1}	ν_{C2H2}	ν_{H2}	ν_{CO}	Q_{CR} (J/kmol)
cyclohexane	C_6H_{12}	1	3	3	0	8.03e+08
n-Heptane	C_7H_{16}	1	3.5	4.5	0	9.82e+08
Iso-Octane	C_8H_{18}	1	4	5	0	1.13e+09
Ethanol	C_2H_6O	1	0.5	2.5	1	2.98e+08

The temperature at which cracking occurs determines the location of the cracking sheet. Based on species and temperature data for a Wolfhard-Parker slot burner [12], the cracking temperature was chosen to be 1350 K. This temperature corresponds to the location of the peak concentration of acetylene.

The ambient parameters are given in table 4. All values are taken for air at the ambient temperature except the specific heat and the Prandtl number. The specific heat was chosen so that the theoretical temperatures do not exceed the adiabatic flame temperature for the fuel. As a reference, this value of specific heat corresponds to the specific heat of air at about 2200 K. The presence of species related to combustion

might explain the high value of the specific heat. The Prandtl number was increased to 0.73 to account for products in system. The dimensionless numbers which control the diffusion flame are given in table 5. The definitions for the dimensionless numbers are given in table 1. For the mass transfer number, the latent heat includes the heat required to bring the liquid fuel from the initial reservoir temperature to the boiling temperature. The data for the nondimensional numbers were taken from the CRC Handbook of Chemistry and Physics [13].

The flame model was run with and without cracking. For the case without cracking, Q was set equal to zero and h_{cr} was set equal to the flame enthalpy. The resulting solution is equivalent to the case without cracking. The temperature dependent density viscosity was used for all runs.

Table 4
Values of Ambient Parameters

Pr	0.73
Y_o	0.232
T	288 K
v	1.46×10^{-5} m / s^2
c_p	1405 J / (kg K)

Table 5
Dimensionless Flame Controlling Numbers

fuel	Φ_{FT}	B	$\tilde{h}_v$	$\tilde{h}_{cr}$	$\tilde{Q}$	Gr_l
cyclohexane	14.7	5.24	0.032	0.50	0.22	1.08×10^{10}
n-heptane	15.1	4.50	0.040	0.50	0.22	1.37×10^{10}
iso-octane	15.1	4.95	0.041	0.50	0.22	1.37×10^{10}
ethanol	8.98	3.04	0.030	0.50	0.24	1.03×10^{10}

It is useful to collapse the experimental measurements taken at different locations downstream onto a single graph through the use of a similarity variable. The analysis predicts that the boundary layer will grow proportional to the fourth root of downstream location. The similarity variable used in the analysis includes the Horwarth transform which distorts the shape of the profiles and is unsuitable for use with experimental data. A similarity variable which can be determined from experimental measurements alone is defined as

$$\eta_{exp} \equiv \frac{x}{x^{1/4}} . \qquad (70)$$

and is consistent with the analysis. The analysis predicts that the streamwise velocity will grow proportional to the square root of downstream location. The similar velocity is defined as

$$U_{sim} \equiv \frac{u}{\sqrt{x}} . \qquad (71)$$

To represent the pyrolysis rate at the wall a nondimensional mass flux is introduced. From the similar stream function and the nondimensional normal velocity, the nondimensional mass flux is defined as

$$\tilde{\dot{m}}''' \equiv \frac{\sqrt{2}\, \ell\, \xi^{1/4}\, \dot{m}(\xi)}{3\, \rho_\infty\, \nu_\infty\, Gr_\ell^{1/4}} = -f(0) . \qquad (72)$$

B. Experimental Results

The results for temperature and streamwise velocity fields are given in figures 2 through 9 using the flame controlling numbers given in tables 5 and the ambient properties in table 4. The experimental data were taken from reference [2]. The curves labeled one step represent the solution to the problem without thermal cracking. The curves labeled two step represent the solution of the problem including the effects of cracking. The data points labeled in centimeters indicate at what location downstream the data was measured at.

In general, the inclusion of thermal cracking significantly improves the agreement between theoretical and experimental results. The temperature profiles with the effect of cracking exhibit remarkable agreement with experimental. For ethanol, n-heptane, and iso-octane, the predicted flame location and the experimental flame location agree to within 2%. For cyclohexane the predicted flame location was off by about 10%. For the solutions without cracking, the flame locations were off by at least 25%. The shape of the theoretical temperature curves with thermal cracking gives a much better fit to the experimental results then the temperature curves without cracking. The improvement is particularly evident in the temperatures next to the wall. The analytical model predicts that the cracking sheet will appear as a kink in the temperature profile. The experimental temperatures do not show any sort of kink. This sugests that the cracking reaction must occur over a wide range of temperatures and should not, in general, be confined to a sheet. The advantage of the cracking sheet is that it makes the solution far more

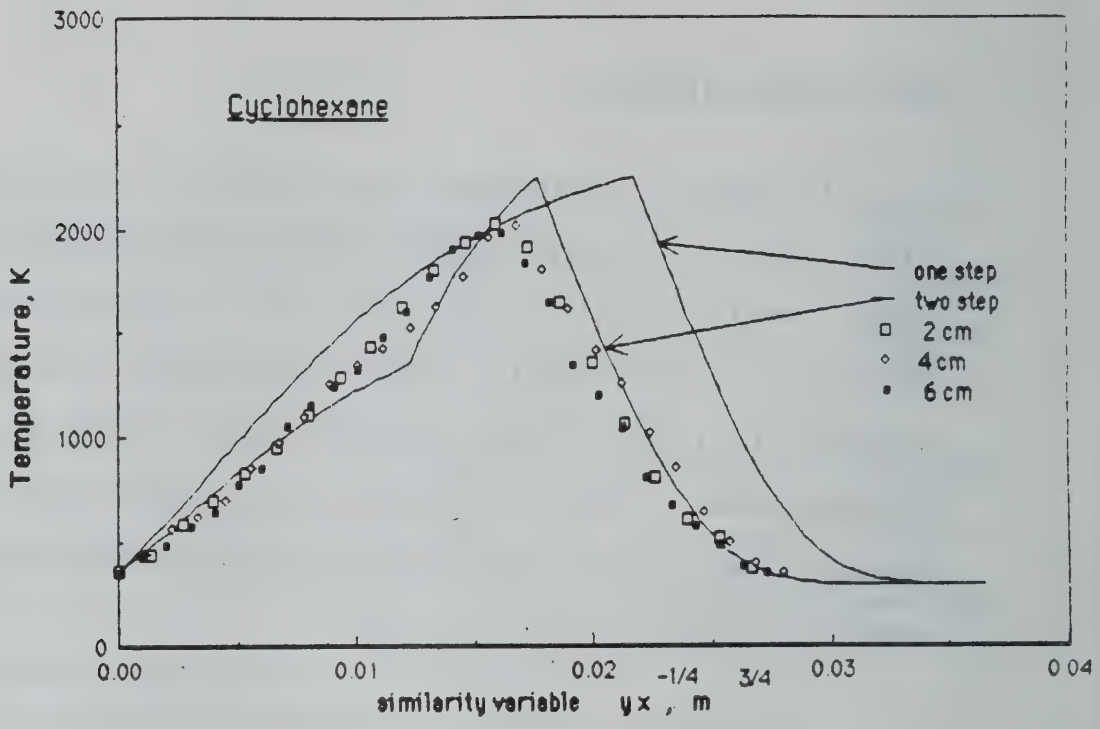
Cyclohexane
Temperature, K
3000
2000
1000
0
0.00
0.01
0.02
0.03
0.04
one step
two step
2 cm
4 cm
6 cm
similarity variable y x , m
-1/4
3/4

Fig. 2

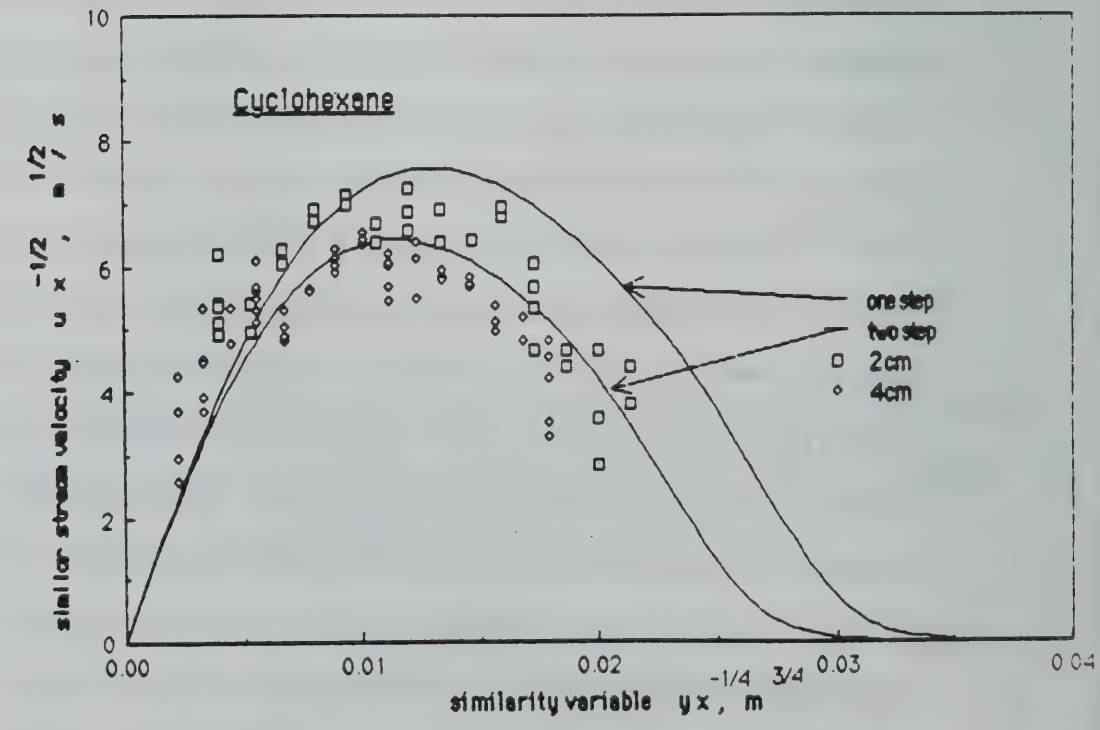
Cyclohexane
similar stream velocity u x , m / s
-1/2
1/2
10
8
6
4
2
0
0.00
0.01
0.02
0.03
0.04
one step
two step
2cm
4cm
similarity variable y x , m
-1/4
3/4

Fig. 3

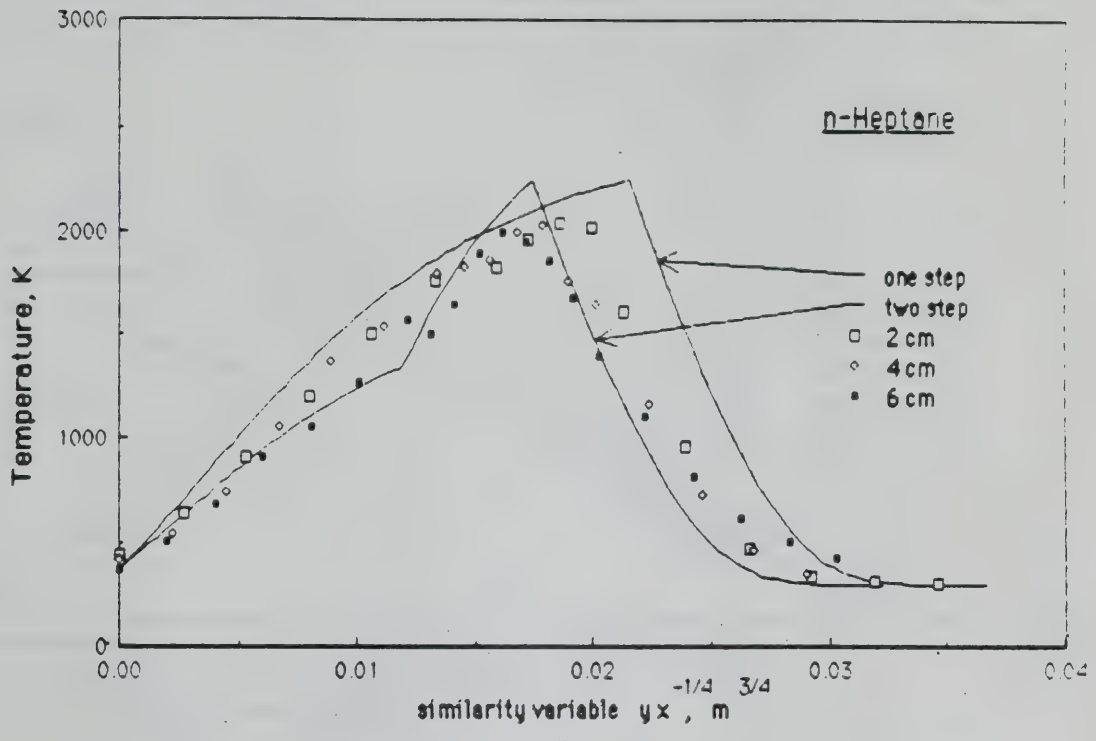
n-Heptane
Temperature, K
3000
2000
1000
0
0.00
0.01
0.02
0.03
0.04
one step
two step
2 cm
4 cm
6 cm
similarity variable y x , m
-1/4 3/4

Fig. 4

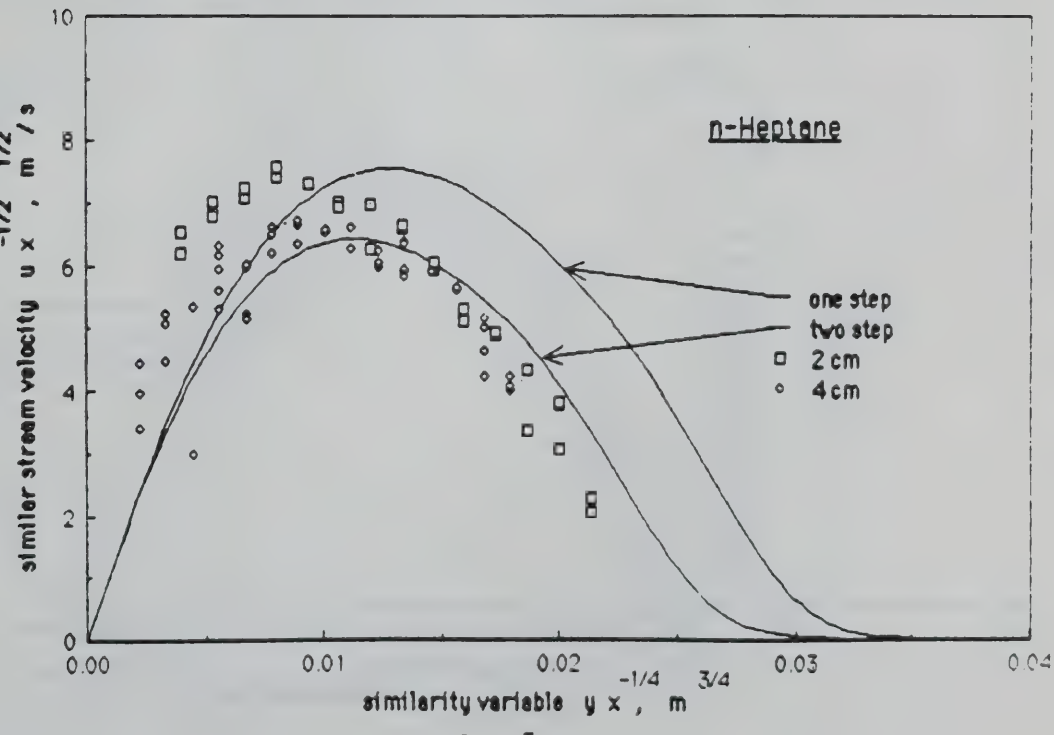
n-Heptane
similer stream velocity u x , m / s
-1/2 1/2
10
8
6
4
2
0
0.00
0.01
0.02
0.03
0.04
one step
two step
2 cm
4 cm
similarity variable y x , m
-1/4 3/4

Fig. 5

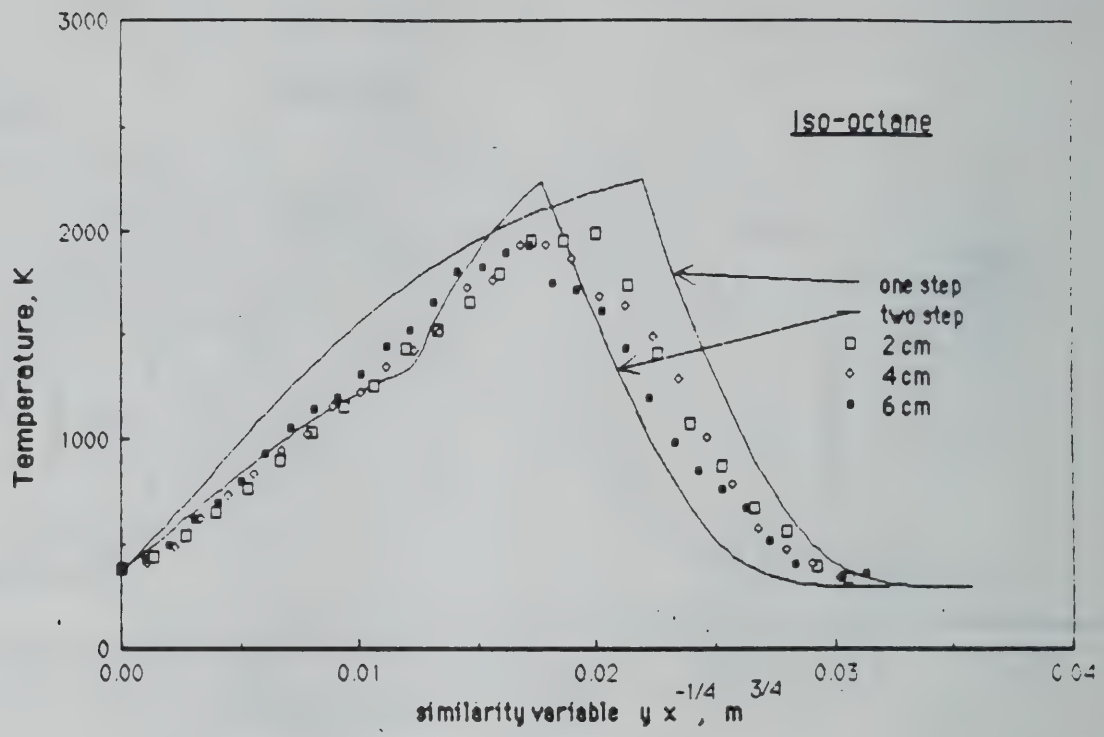
Iso-octane
Temperature, K
3000
2000
1000
0
0.00
0.01
0.02
0.03
0.04
one step
two step
2 cm
4 cm
6 cm
similarity variable y x , m
-1/4 3/4

Fig. 6

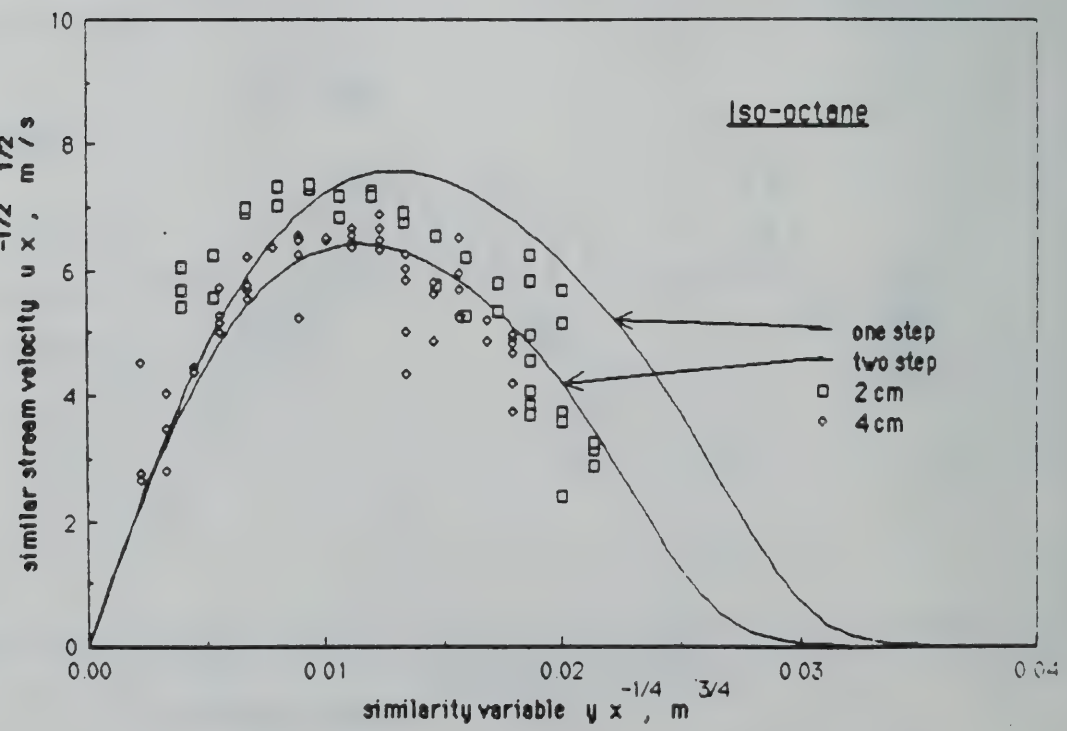
Iso-octane
similar stream velocity u x , m / s
-1/2 1/2
10
8
6
4
2
0
0.00
0.01
0.02
0.03
0.04
one step
two step
2 cm
4 cm
similarity variable y x , m
-1/4 3/4

Fig. 7

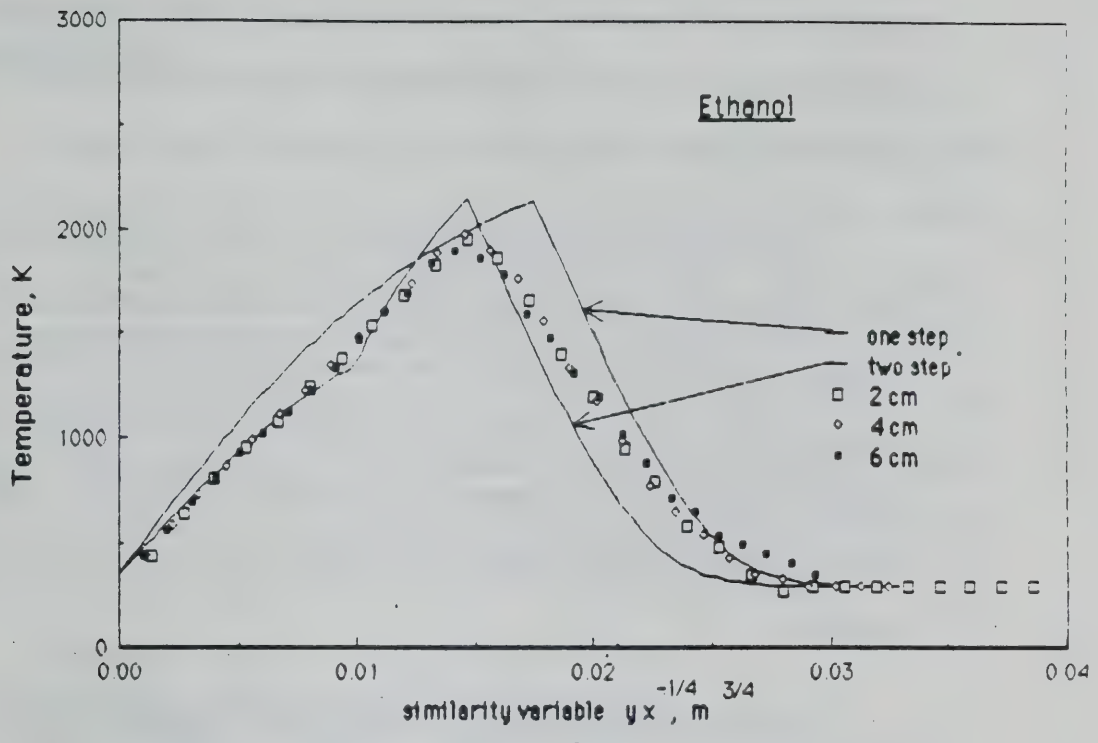
Ethanol
Temperature, K
3000
2000
1000
0
0.00
0.01
0.02
0.03
0.04
similarity variable y x , m
-1/4 3/4
one step
two step
2 cm
4 cm
6 cm

Fig. 8

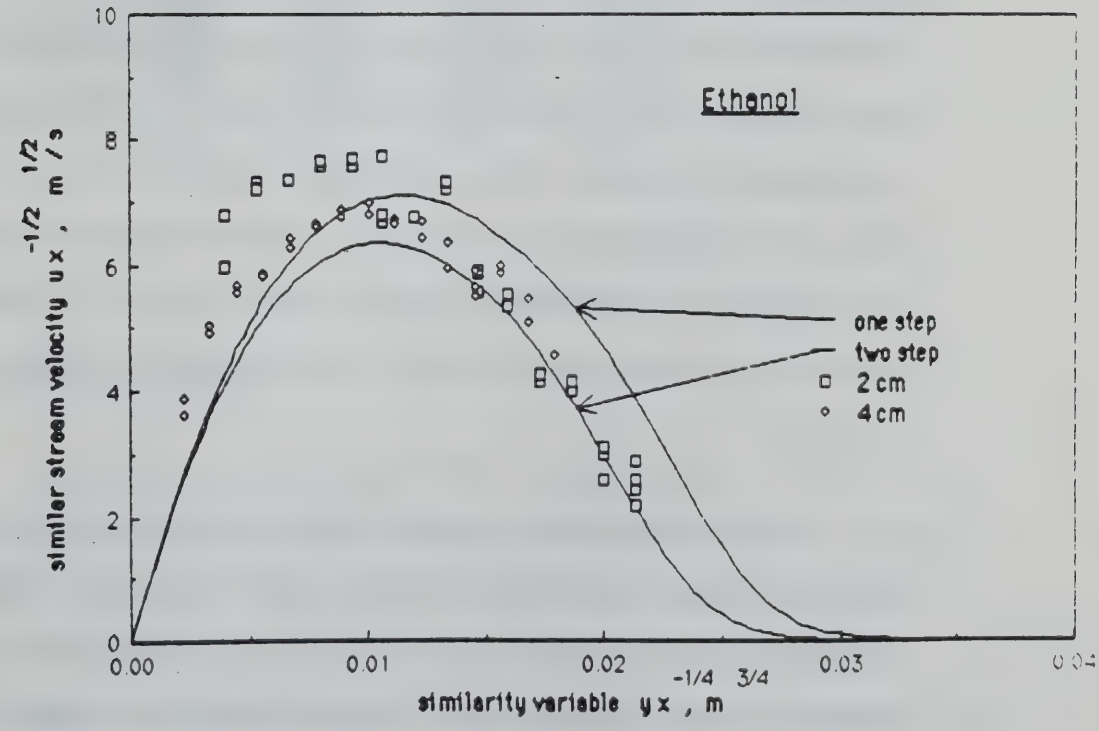
Ethanol
similar stream velocity u x , m / s
-1/2 1/2
10
8
6
4
2
0
0.00
0.01
0.02
0.03
0.04
similarity variable y x , m
-1/4 3/4
one step
two step
2 cm
4 cm

Fig 9

tractable and is therefore, a useful idealization. The flame is well represented by a sheet. The experimental temperatures show a distinct peak at the flame.

The density of the gases between the wall and the flame have a strong influence on the flame location due to the appearance of density in the Horwarth transformation. The lower temperatures between the wall and the flame cause the flame to move toward the wall due to the increase in density of the gases in this region. This is the main reason why the location of the flame moves closer to the wall with the addition of cracking.

The lower temperatures between the flame and the wall have a strong influence on the velocity profiles since the flow is buoyancy driven. The inclusion of cracking reduces the peak velocity by about 15 %. Agreement is improved with velocities on the edge of the boundary layer but theoretical velocities closer to the wall are consistently lower than the experimental velocities. The experimental velocities do not collapse as well as the experimental temperatures. The velocities at two centimeters downstream are much higher than expected. It would be useful to have more velocity measurements further downstream to establish some sort of trend.

The variable properties allow the model to accurately predict the flame location. If the density viscosity product ($\rho\mu$) were taken as a constant and the ambient values were used, the flame location would be moved outward by about 25%. This would destroy the agreement between the theoretical profiles and the experimental profiles.

C. Pyrolysis Rates

The agreement between experimental and theoretical temperatures near the wall should improve the prediction of the pyrolysis rate at the wall since the wall mass flux is determined by the heat transfer to the wall. The dimensionless mass flux at the wall is graphed for each of the fuels in figure 10 comparing the mass flux with and without the cracking reaction. The endothermic cracking reaction reduces the pyrolysis rate at the wall by about 20%. This result is observed in the temperature plots as a decrease in the slope of the temperature profile at the wall.

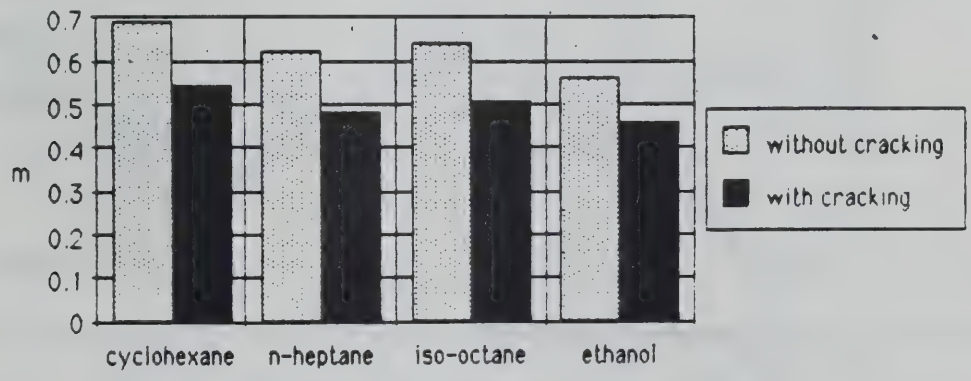

Fig. 10

D. Parametric Studies

Two parametric studies are done using the model to explore how the cracking parameters affect the flame. The dimensionless cracking enthalpy determines where the cracking reaction will occur. Figure 11 shows the results for four different $\tilde{h}_{cr}$ with all of the other flame controlling numbers held constant. Decreasing $\tilde{h}_{cr}$ moves the flame closer to the wall due to the decrease in temperatures between the flame and the wall. In going from $\tilde{h}_{cr}$ = 0.83 to $\tilde{h}_{cr}$ = 0.31 the wall pyrolysis rate

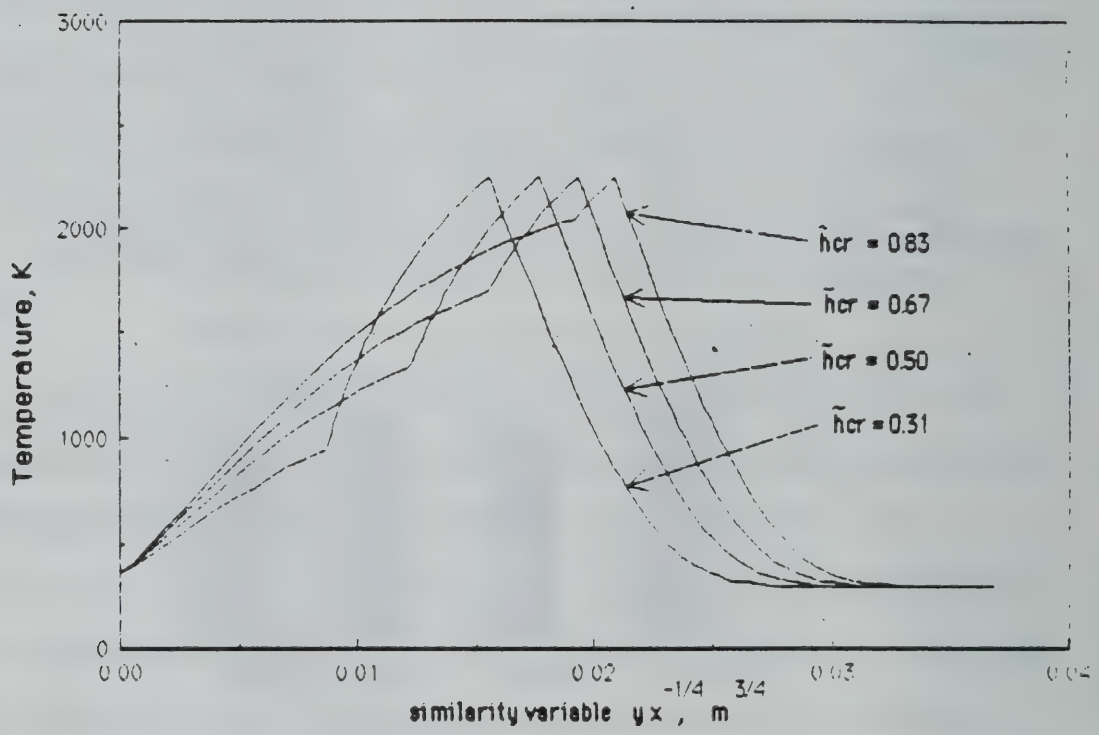
3000
2000
1000
0
Temperature, K
0 00
0 01
0 02
0 03
0 04
similarity variable y x , m
-1/4 3/4
h̃cr = 0.83
h̃cr = 0.67
h̃cr = 0.50
h̃cr = 0.31

Fig. 11

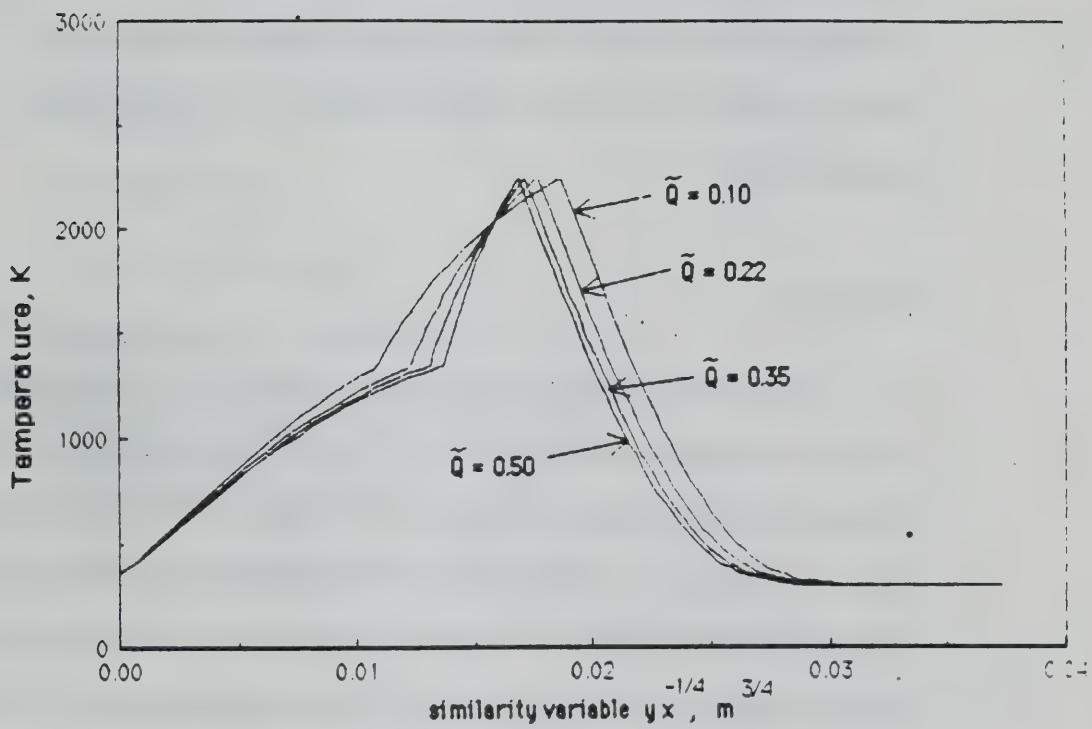
3000
2000
1000
0
Temperature, K
$\tilde{Q}$ = 0.10
$\tilde{Q}$ = 0.22
$\tilde{Q}$ = 0.35
$\tilde{Q}$ = 0.50
0.00
0.01
0.02
0.03
similarity variable $yx^{-1/4}$, m$^{3/4}$

Fig. 12

drops more than 30 %. This is indicated by the decrease in the slope of the temperature profile at the wall.

Figure 12 shows the effect of changing $\tilde{Q}$ on the temperature profiles. Increasing $\tilde{Q}$ moves the flame closer to the wall and causes the kink in the temperature profile to become more pronounced. As $\tilde{Q}$ increases, the heat flux to the cracking sheet must increase. This causes the temperature profile to become steeper on the flame side of the cracking sheet.

Conclusion

Endothermic cracking of fuel and temperature dependent density-viscosity product were added to the free convective boundary layer diffusion flame solution presented by Pagni[2]. With the addition of thermal cracking, the agreement between experimental and theoretical and experimental results are greatly improved. The pyrolysis rate at the wall is reduced due the existence of the endothermic cracking sheet. The use of temperature dependent density-viscosity product enables the flame model to accurately predict the location of flame. Future work would include adding radiation to the model or applying the model to other types of diffusion flames.

Nomenclature

Capital Letters

B	Spaldings mass transfer number, eqn. (36)
B_{cr}	Cracking mass transfer number, eqn. (39)
B_{eff}	Effective B number which accounts for cracking, eqn. (40)
D	Diffusivity
F_1	Uncracked fuel
F_2	Cracked fuel molecule
Gr_l	Grashof number evaluated at x = 1 m
J	Solution to energy-species equation
J_{cr}	Value of J at crack sheet, eqn. (43)
J_{fl}	Value of J at flame sheet, eqn. (45)
L	Latent heat of vaporization for pyrolyzed material
Le	Lewis number
M_f	Molecular weight of uncracked fuel
O	Oxygen O_2
P	General term for products
Pr	Prandtl number
$\tilde{Q}$	Heat of reaction ratio, eqn.(34)
Q_{fl}	Heat of reaction for one step reaction
Q_{cr}	Heat of reaction for cracking reaction
Q_{crfl}	Heat of reaction for combustion of cracked fuel, eqn. (4)
T	Temperature

T_r Temperature of fuel reservoir

T_w Wall temperature

T_{cr} Temperature at which cracking occurs

T_∞ Ambient temperature

U Nondimensional streamwise velocity

V Nondimensional transverse velocity

Y_{f1} Mass fraction of uncracked fuel

Y_{f2} Mass fraction of cracked fuel

Y_{f2w} Mass fraction of cracked fuel at wall

Y_{f1w} Mass fraction of uncracked fuel at wall

Y_{ft} Mass fraction of fuel in pyrolyzed material from wall

Y_o Mass fraction of oxygen

Y_o Ambient mass fraction of oxygen

Small Letters

c_p Specific heat

f Similar part of stream function

h Enthalpy

$\tilde{h}$ Dimensionless enthalpy, eqn.(34)

$\tilde{h}_{cr}$ Dimensionless enthalpy at crack sheet, eqn.(44)

$\tilde{h}_w$ Dimensionless enthalpy at wall, eqn.(36)

ℓ Arbitrary length, set equal to 1 m

$\dot{m}''_w$ Mass flux at wall

$\dot{m}'''$	Mass generation term
$\tilde{\dot{m}}''$	Dimensionless mass flux at wall, eqn. (73)
n	Normal to wall
p	Pressure
u	Streamwise velocity
$\sim$	Transverse velocity
w	Evaluated at wall
x	Streamwise coordinate
y	Transverse coordinate
$\tilde{y}_{f1}$	Dimensionless uncracked fuel, eqn.(23A)
$\tilde{y}_{f2}$	Dimensionless cracked fuel, eqn.(23B)
$\tilde{y}_{o}$	Dimensionless oxygen, eqn.(23C)
$\tilde{y}_{f2CR}$	Dimensionless cracked fuel at cracking sheet, eqn.(44)

Greek Symbols

$\propto$	Temperature dependent density viscosity function, eqn.(49)
ϕ_{FT}	Dimensionless fuel in transferred gas, eqn.(37)
ϕ_{F1}	Dimensionless uncracked fuel equivalence ratio, eqn.(24)
ϕ_{F2}	Dimensionless cracked fuel equivalence ratio, eqn.(25)
ν	Stoichiometric coefficient
ρ	Density
μ	Dynamic viscosity
ν_{∞}	Kinematic viscosity at ambient
λ	Thermal condictivity

ξ	Nondimensional streamwise coordinate, eqn.(52A)
ζ	Nondimensional transverse coordinate, eqn.(52B)
ψ	Nondimensional stream function, eqn.(57)
λ	Nondimensional similarity variable, eqn.(58)

Subscripts

CR	Evaluated at cracking sheet
FL	Evaluated at flame
f	Uncracked fuel
f1	Uncracked fuel
f2	Cracked fuel
o	Oxygen
p	Products
w	Evaluated at wall
	Evaluated at infinity

Superscripts

$\cdot$	Per unit time
$'$	Per unit length or derivative with respect to the independent variable

VI. Figure Captions

Figure 1. Schematic diagram of free convective boundary layer diffusion flame showing internal parts and coordinate system.

Figure 2 Temperature results for cyclohexane. Experimental temperature data is compared with theoretical results for the model with and without cracking . The curve labeled "one step" indicates the solution without cracking. The curve labeled "two step" indicates the solution including the effects of cracking. Experimental data is taken from three locations downstream. The use of a similarity variable, eqn.(73), allow the data to be plotted on a single graph. The data labeled 2 cm indicates that the experimental data was measured 2 cm downstream from the leading edge of the flame. The points labeled 4 cm and 6 cm are experimental date taken at four and six centimeters downstream.

Figure 3 Streamwise velocity results for cyclohexane. Experimental streamwise velocity data is compared with theoretical results for the model with and without cracking. The curve labeled "one step" indicates the solution without cracking. The curve labeled "two step" indicates the solution includes the effects of cracking. Experimental data is taken from two locations downstream. The use of a similarity variable, eqn.(73), and a similar velocity, eqn.(74), allow the data to be plotted on a single graph. The points labeled 2 cm and 4 cm are experimental date taken at two and four centimeters downstream from leading edge of flame.

Figure 4 Temperature results for n-heptane. Symbols and curves are defined as in figure 2.

Figure 5 Streamwise velocity results for n-heptane. Symbols and curves are defined as in figure 3.

Figure 6 Temperature results for iso-octane. Symbols and curves are defined as in figure 2.

Figure 7 Streamwise velocity results for iso-octane. Symbols and curves are defined as in figure 3.

Figure 8 Temperature results for ethanol. Symbols and curves are defined as in figure 2.

Figure 9 Streamwise velocity results for ethanol. Symbols and curves are defined as in figure 3.

Figure 10 The value of the dimensionless mass flux at the wall is graphed for each of the fuels for the flame with and without thermal cracking.

Figure 11 Influence of h_{cr} on temperature profiles. The cracking temperatures are as follows: $\tilde{h}_{cr} = 0.83$, Tcr = 2050 ; $\tilde{h}_{cr} = 0.67$, Tcr = 1700 ; $\tilde{h}_{cr} = 0.50$, Tcr = 1350 ; $\tilde{h}_{cr} = 0.31$, Tcr = 950 . The other flame controlling numbers were held constant. ϕ_{FT} = 14.7, B = 5.24, $\tilde{h}_w = 0.03$, $\tilde{Q} = 0.22$, $Gr_l = 1.08 \times 10^{10}$.

Figure 12 Influence of Q on temperature profiles.The other flame controlling numbers were held constant. $\phi_{FT} = 14.7$, B = 5.24, $\tilde{h}_w = 0.03$, $\tilde{h}_{cr} = 0.50$, $Gr_l = 1.08 \times 10^{10}$.

VII. References.

1. Pagni, P.J., "Diffusion Flame Analysis," Fire Safety Journel, Vol. 3, 1980/81, pp. 273-285.

2. Ang, J.A. ; Pagni , P.J. ; Mataga, T.G. ; Margle, J.M. , and Lyons, V.J. , "Temperature and Velocity Profiles in Sooting Free Boundary Layer Flames," AIAA Journal, submitted, 1986.

3. Kosdon, F. J., Willeams, F. A., and Buman, C., "Combustion of Verticla Cellulosic Cylinder in Air," *Twelfth Symposium (Int'l) on Combustion*, pp. 253-264, The Combustion Institute, 1969.

4. Kim, J. S., deRis, J., and Krosser, F. W., "Laminar Free-Convective Burning of Fuel Surface," *Thirteenth Symposium (Int'l) on Combustion*, pp. 949-961, The Combustion Institute, 1971.

5. Nakagawa, Y., Nishiwaki, N., and Hirata, M., "Effect of Combustion on a Laminar Boundary Layer," *Thirteenth Symposium (International) on Combustion*, The Combustion Institute, 1971, pp. 813-819.

6. Andreussi, P., and Petarca, L., "Film Combustion of Ethly Alcohol in a Parallel Air Stream," *Eighteenth Symposium (International) on Combustion*, The Combustion Institute, 1981, pp. 1861-1869.

7. Ramachandra, A., and Raghunandan, B.N., "An Analysis of a Boundary Layer Diffusion Flame Over a Porous Flat Plate in a Confined Flow," Combustion science and Technology, Vol. 38, 1984, pp 59-73.

8. Penner, S. S. , and Libby, P.A., "Convective Laminar Heat Transfer with Combustion for a Lewis Number of Unity," Astronautica Acta, Vol. 13, 1967, pp. 75-91.

9. Fay, J. A., Riddell, F. R., "Theory of STagnation Point Heat Transfer in Dissociated Air," Journal of the Aeronautical Sciences, Vol. 25, February, 1958.

10. Okoh, C.I. , "Soot and Radiation in Free Boundary Layer Flames," Ph.D. Thesis, ucb , 1984.

11. Hirschfelder, J. O. Curtiss, C.F., and Bird, B. R. , Molecular Theory of Gases and Liquids, John Wiley and Sons, New York, 1964.

12. Smyth, K. C., Miller, J. H., Dorfman, R. C., Mallard, W. G., and Santoro, R. J., "Soot Inception in a Methane/Air Diffusion Flame as Characterized by Detailed Species Profiles," Combustion and Flame, 62:157 (1985).

13. Weast, R. C., CRC Handbook of Chemistry and Physics, CRC Press, Inc., West Palm Beach, 1978.

FORM NBS-114A (REV.11-84)

U.S. DEPT. OF COMM. BIBLIOGRAPHIC DATA SHEET (See instructions)	1. PUBLICATION OR REPORT NO. NBS/GCR-88/542	2. Performing Organ. Report No.	3. Publication Date March 1988

4. TITLE AND SUBTITLE

Thermal Cracking and Variable Properties Effects on Free Boundary Layer Diffusion Flames

5. AUTHOR(S)

Thomas George Matage

6. PERFORMING ORGANIZATION (If joint or other than NBS, see instructions)

University of California
Berkeley, CA

7. Contract/Grant No.
60NANB5D0552

8. Type of Report & Period Covered

9. SPONSORING ORGANIZATION NAME AND COMPLETE ADDRESS (Street, City, State, ZIP)

National Bureau of Standards
U.S. Department of Commerce
Gaithersburg, MD 20899

10. SUPPLEMENTARY NOTES

☐ Document describes a computer program; SF-185, FIPS Software Summary, is attached.

11. ABSTRACT (A 200-word or less factual summary of most significant information. If document includes a significant bibliography or literature survey, mention it here)

This paper presents an analytical model for a free convective boundary layer diffusion flame and compares results from this model to experiment. The analytical model will add two new features to the solution presented by Pagni in order to improve agreement with experimental data. It is proposed that the fuel undergoes endothermic decomposition before reaching the flame. The endothermic decomposition of the fuel will be referred to as cracking. The effect of cracking on the free convective diffusion flame is explored by the use of modified Shvab Zeldovich variables which model both the flame reaction and the cracking reaction. The second addition to the solution given by Pagni is the use of a temperature dependent density-viscosity function which allows the ambient viscosity to be determined by ambient conditions. In order to match the location of the theoretical flame with the location of the experimental flame, previous studies have adjusted the ambient viscosity to non ambient values. By using the temperature dependent density-viscosity function, the analytical model accurately predicts the location of the flame using the ambient value of viscosity.

12. KEY WORDS (Six to twelve entries; alphabetical order; capitalize only proper names; and separate key words by semicolons)

boundary layers; cracking (fracturing); diffusion flames; flame spread; mathematical models

13. AVAILABILITY

☒ Unlimited
☐ For Official Distribution. Do Not Release to NTIS
☐ Order From Superintendent of Documents, U.S. Government Printing Office, Washington, DC 20402.
☒ Order From National Technical Information Service (NTIS), Springfield, VA 22161

14. NO. OF PRINTED PAGES
45

15. Price
$11.95